

Research Article

Study on Spatio-temporal Distribution of Chlorophyll-a on Pelagic Catch Productivity in Muara Bendera, West Java, Indonesia

Heri Setiawan^{1,2} , Masita Dwi Mandini Manessa^{1*} , and Supriatna¹ 

¹Department of Geography, Faculty of Mathematics and Natural Sciences, University of Indonesia, Depok, West Java. Indonesia
²Geospatial Information Agency, Bogor, West Java. Indonesia



ARTICLE INFO

Received: March 12, 2024
Accepted: June 02, 2024
Published: June 19, 2024
Available online: Oct 23, 2024

*) Corresponding author:
E-mail: manessa@ui.ac.id

Keywords:
Chlorophyll-a
Productivity
Pelagic
Spatiotemporal
Spatial Trend
Indonesia



This is an open access article under the CC BY-NC-SA license (<https://creativecommons.org/licenses/by-nc-sa/4.0/>)

Abstract

Chlorophyll-a has been considered an indicator of pelagic fish abundance in waters. Although a high nutrient load causes eutrophication, leading to fish mortality, global-scale climate anomalies will also influence the oceanographic conditions of the seas. This study aimed to investigate spatial patterns and trends of chlorophyll-a, the relationship between chlorophyll-a and pelagic fish catch productivity, and the effect of ENSO and IOD on pelagic fish catch productivity. The chlorophyll-a data were obtained from the SeaWiFS and Terra-Aqua MODIS time-series datasets of ocean color satellites. The results indicated that Jakarta Bay had the highest chlorophyll-A concentration. The Chlorophyll-A concentrations declined as the distance between the estuary and the coast grew. From 1997 to 2021, the regional pattern of increasing chlorophyll-a concentrations in the Citarum and Cisdane estuaries was continuous. Since 2001, the concentration of chlorophyll-a in Jakarta Bay has declined, whereas it has begun to climb in the seas of the North Seribu Islands. The increasing chlorophyll-A trend in the Seribu Islands is attributed to rising nitrate levels induced by human-driven coral degradation. Between 1997 and 2021, the concentration of chlorophyll-a in the Muara Bendera fishing region grew by +0.013 mg/m³/year, or 1.43 percent each year. The correlation between chlorophyll-a and pelagic fish catch productivity was -0.13. ENSO does not affect the productivity of pelagic catches in this region. However, it was discovered that IOD reduced the productivity of low-category pelagic catches.

Cite this as: Setiawan, H., Manessaa, M. D. M., & Supriatna. (2024). Study on Spatio-temporal Distribution of Chlorophyll-a on Pelagic Catch Productivity in Muara Bendera, West Java, Indonesia. *Jurnal Ilmiah Perikanan dan Kelautan*, 16(2):349–363. <https://doi.org/10.20473/jipk.v16i2.55940>

1. Introduction

Chlorophyll-a is the primary pigment of phytoplankton, which has been considered to reflect the abundance of pelagic fish in water whose existence is affected by pollution and climate change. The main pigment used by phytoplankton to capture light energy and convert this energy into biomass is known as chlorophyll-a (Jakobsen and Markager, 2016). Fish catch areas can be predicted with high concentrations of chlorophyll-a because it has been proven that chlorophyll-a has a strong to very strong correlation with the number of catches of pelagic fish such as mackerel (Welliken *et al.*, 2018), small pelagic fish (Tangke and Senen, 2020), and male mackerel (Tangke *et al.*, 2021). Estuaries are productive environments used by many fish as nurseries (James *et al.*, 2019) and whose existence is influenced by abiotic, biotic, and anthropogenic factors (Rodrigues *et al.*, 2019). The sustainability of fish habitats is affected by climate change, built infrastructure, destructive fishing practices, and pollution. The chlorophyll-a level is influenced by nutrient supply and global climate anomalies (Hu *et al.*, 2021).

Annually, Citarum River pollution causes eutrophication to trigger the occurrence of an algae bloom, which can disturb and even cause the death of fish habitats in the Muara Bendera catchment area. Muara Bendera Fishing Port is located in the Citarum River Estuary, Pantai Bahagia Village, Muara Gembong District, Bekasi Regency, West Java. Muara Gembong waters have poor water quality and continue to decline every year due to pollution of the Citarum River (Nastiti *et al.*, 2020; Ihsan *et al.*, 2023), the sources of which come from industrial waste, households, agriculture, animal husbandry, fisheries, and other activities (Ramadhiani and Suharyanto, 2021; Sholeh *et al.*, 2018). About 3,000 industries dump their waste into the Citarum River (Sembiring *et al.*, 2020), and, as a result of this, several fish species have died in the river's reaches of the Citarum River. The increased nutrient load in estuaries will impact the risk of eutrophication (Yu *et al.*, 2018). Nutrients Nitrate (N) and Phosphate (P) will increase the algae biomass of a body of water, including phytoplankton (Van Meerssche and Pinckney, 2019). Furthermore, many dead algae will settle at the bottom of the waters and be decomposed by bacteria into inorganic material that requires much oxygen, resulting in oxygen levels decreasing drastically (Devlin and Brodie, 2023). Even in the worst conditions, when anoxia occurs, the cessation of oxygen intake causes the death of fish (Pitcher and Jacinto, 2020). This phenomenon, known as algae bloom, once occurred in the waters of Jakarta Bay during the dry season of 2014–2015, which is the

catchment area of Muara Bendera fish. Algae bloom due to biomass accumulation in the aquatic column is due to high nutrient factors, sufficient sunlight, and minimal currents (Ajani *et al.*, 2018).

Climate variability in Indonesia will affect the primary productivity of the waters. Global climate change will affect oceanographic conditions or the aquatic environment (Ghosh *et al.*, 2021). The climate in Indonesia is influenced by El Niño Southern Oscillation (ENSO) and Indian Ocean Dipole (IOD), and there has been a shift in fish catchment areas in the Java Sea throughout the year due to the influence of the seasons (Apriansyah *et al.*, 2023). Some marine species' catches are influenced by climate variations, especially El Niño, sea surface temperatures, and high rainfall (Alms and Wolff, 2020). Seabed water will flow upwards, forming upwelling areas essential to high-productivity fishing grounds (Hsiao *et al.*, 2021), as phytoplankton will take nutrients from upwelling (Paparazzo *et al.*, 2021). IOD will increase the abundance of small pelagic fish in Indian Ocean waters, including the southern waters of Java, during the upwelling process (Lumban-Gaol *et al.*, 2021).

As a consequence of this pollution in the waters, the number of Muara Bendera fishermen caught has decreased. Muara Gembong waters have poor water quality and continue to decline, but they remain the mainstay for fishermen to find fish (Ihsan *et al.*, 2023). According to Pantai Bahagia Village fishermen, in the late 1990s, the Citarum River Estuary was still in its prime. However, after the turn of the century, fish catches began to decline. As fish nurseries, mangroves will be harmed by solid waste pollution, while black and putrid liquid waste causes massive fish deaths (Akram *et al.*, 2023).

Remote sensing data can be used for oceanographic monitoring information, including chlorophyll-a as input for fisheries resource management. Some of the multispectral images that have been used in research to obtain chlorophyll-a information in waters include SeaWiFS (Haridhi *et al.*, 2018), Terra MODIS (Daqamseh *et al.*, 2019; Yin *et al.*, 2021), Aqua MODIS (Ciancia *et al.*, 2018; Daqamseh *et al.*, 2019; Muskananfolo *et al.*, 2021), MERIS (Attila *et al.*, 2018), Landsat (Fu *et al.*, 2018; Mukhtar *et al.*, 2021; Poddar *et al.*, 2019), and Sentinel (Poddar *et al.*, 2019; Vanhellemont and Ruddick, 2021). Aqua MODIS and Terra MODIS are the solutions for monitoring oceanographic conditions because they have an excellent temporal resolution of one day, as do SeaWiFS. Using these three data that can monitor water quality, such as (chlorophyll-a) with a fairly wide spatial range through harmonization of reflectance values, is interesting to obtain a broader chlorophyll-a time series.

In addition, creating a spatial trend model of chlorophyll-a is needed to analyze its changes. Assessing chlorophyll-a and its impacts is critical to evaluating the resilience of marine biodiversity (Ser-Giacomi *et al.*, 2018). In addition, it can be used to evaluate environmental status in marine spatial planning, such as for marine conservation areas and sectoral licensing (Tweddle *et al.*, 2018). However, all previous research focused on describing the use of remote sensing for water quality mapping, whereas this research thoroughly examines the spatial patterns and trends of chlorophyll-a and its relationship with pelagic fish abundance. Beyond the conventional understanding of this connection, the study delves into the influence of global-scale climate anomalies such as ENSO and IOD on these ecological dynamics. Through detailed investigation, the study identifies specific concentrations of chlorophyll-a in different regions, with Jakarta Bay standing out as a key area with the highest levels. Additionally, temporal trends are uncovered, including a decrease in chlorophyll-a concentration in Jakarta Bay since 2001 and an increase in the North Seribu Islands linked to human activities. This study aims to analyze chlorophyll-a's spatial patterns and trends in 1997 - 2021, the correlation between chlorophyll-a and pelagic fish productivity, and the influence of ENSO and IOD phenomena on the productivity of pelagic fish in the Muara Bendera fishing area.

2. Materials and Methods

2.1 Materials

The materials used in this study are SeaWiFS, Terra MODIS, and Aqua MODIS level 3 monthly; ONI data; DMI data; and fish catch data. The equipment used is a Dell Latitude E5470 Laptop that can run the Google Earth Engine platform, ArcGIS 10.8 software, and R Studio software version 4.1.1.

2.1.1 Ethical approval

This study does not require ethical approval because it does not use experimental animals.

2.1.2 Chlorophyll-a data of SeaWiFS, terra MODIS, and aqua MODIS

Chlorophyll-a was obtained from SeaWiFS, Terra MODIS, and Aqua MODIS level 3 monthly from the Ocean Biology Processing Group - National Aeronautics and Space Administration (OBPG-NA-SA). Level 3 MODIS and SeaWiFS are stored at a resolution of 4.6 km and 9.2 km. Based on NASA, chlorophyll-a is obtained using a global algorithm, which is a combination of the OC3/OC4 ratio band (OCx) algorithm from O'Reilly with the Color Index

(CI) Algorithm from (Hu *et al.*, 2012). Chlorophyll retrieval at $<0.15 \text{ mg/m}^3$ was using the CI algorithm, and chlorophyll retrieval $>0.2 \text{ mg/m}^3$ using the OCx algorithm. Taking chlorophyll between the two values was performed using a combination of CI and OCx algorithms with a weighting approach. The time series uses SeaWiFS data from October 1997 – February 2000, Terra MODIS from March 2000 – December 2002, and Aqua MODIS from January 2003 – December 2021. Meanwhile, the data for processing spatial distribution and spatial trend models uses SeaWiFS October 1997 – December 2000, Terra MODIS March 2001 – December 2021, and Aqua MODIS January 2011 – December 2021.

The accuracy of the global algorithm is assessed using bias and mean absolute error (MAE) values, following the recommendation of Seegers *et al.*, (2018). MAE accurately reflects the magnitude of errors with spatial and temporal consistency, while bias values estimate systematic errors. Typically, model accuracy calculations involve root mean square (RMSE) and determination value (R^2), but both are not recommended. RMSE depends heavily on the number and distribution of validation samples, and R^2 is inflated by random errors. According to the ocean color website, SeaWiFS has a bias value of 1.02610, Terra MODIS of 1.09015, and Aqua MODIS of 1.18374. MAE values for SeaWiFS, Terra MODIS, and Aqua MODIS are 1.64047, 1.67414, and 1.67632, respectively. For instance, a bias value of 1.02610 indicates that the average model is 2.61% greater than the observed value. The MAE value always exceeds one, so an MAE of 1.64047 indicates a relative measurement error of 64%.

2.1.3 Data on the productivity of pelagic fish catches at the Muara Bendera fishing port

From January 2015 to June 2017, the Fishing Port Information Center, Directorate General of Capture Fisheries, and Ministry of Maritime Affairs and Fisheries successfully collected data on pelagic fish production. Fish that are the object of research include Blackfin barracuda (*Sphyraena qenie*), Indo-Pacific king mackerel (*Scomberomorus guttatus*), Dogtooth tuna (*Gymnosarda unicolor*), black skipjack tuna (*Euthynnus lineatus*), Squaretail mullet (*Liza vaigiensis*), Short mackerel (*Rastrelliger brachysoma*), Savalai hairtail (*Lepturacanthus savala*), and Needlefish (Belonidae).

2.1.4 Oceanic nino index (ONI) data

ENSO monitoring uses ONI data from the National Center for Environmental Prediction - National Oceanic and Atmospheric Administration (NCEP

- NOAA). According to NCEP – NOAA, ONI is an anomaly sea surface temperature NINO3.4 (5°N - 5°S, 120°W-170°W), which is averaged over three months and ends in the current month. Weak El Niño (ONI values of 0.5 to 0.9°C), moderate El Niño (1 to 1.4°C), strong El Niño (>1.5°C); La Nina is weak (ONI values are -0.5 to 0.9°C), La Nina moderate (ONI values are -1 to -1.4°C), La Nina is strong (ONI values are < -1.5°C).

2.1.5 Dipole mode index (DMI) data

IOD monitoring uses DMI data obtained from NOAA (https://psl.noaa.gov/gcos_wgsp/Timeseries/DMI/). The Bureau of Meteorology Australia mentions that DMI is the difference between sea surface temperature between the East Indian Ocean (90° E - 110° E and 10° S - 0° S) and the West Indian Ocean (50° E - 70° E and 10° S - 10° N). The DMI value >0.4°C is a positive phase, <-0.4°C is the negative phase, while the DMI value between the two is the neutral phase.

2.2 Methods

2.2.1 Determination of research areas

The research area is the farthest reach of Muara Bendera fishermen catching fish, as obtained from fishermen's interviews at the Muara Bendera Port. This method was chosen because the typical vessel owned by fishermen is a wooden vessel with a capacity of 5 GT that is not equipped with a global positioning system (GPS), so the ship's coordinate data are unavailable or not archived—considering that this is a small fishing port. This is due to the lack of available equipment, including ships, which becomes an obstacle to data collection. The interview questions emphasize the farthest ranges guided by an island or continent, the length of travel, and the ship's speed. A printed map aids in conducting interviews by making it easier for sources to indicate the location of the fish caught. After completing the interview, the distance was plotted on a map for validation. Generally, the source knows the area of the catch of fellow fishermen because they often meet and gather at the port (van Trijp, 2021). Interview methods depend on the informant's geographic behavior, including psychology and geography knowledge, cognitive geography, and perception. The results of the interview were stated on a map of the research area with the boundaries of the research area at 5° 34' 48.75" S - 5° 59' 28.19" S and 106° 29' 53.57" E - 107° 10' 11.80" E (Figure 1).

2.2.2 Calculation of catch per unit effort (CPUE)

Fish catch productivity reflects the primary productivity of a body of water expressed in Catch Per

Unit Effort (CPUE), defined as follows (Wang et al., 2020):

$$CPEU = C/B \dots \dots \dots (i)$$

Where :

CPUE = catch per unit of effort (ton/operational day)

C = catch (ton)

B = operational day of the catch (operational day)

2.2.3 Chlorophyll-a spatial distribution map generation

The map of the spatial distribution of chlorophyll-a shows the monthly average value of chlorophyll-a obtained from the median value of chlorophyll-a. Then, interpolation of kriging and classification is carried out. The results of the interpolation of chlorophyll-a MODIS kriging show good accuracy can be seen from the R² of in situ data in some waters, such as the waters of Tien Yen Bay Vietnam by 0.78 (Ha et al., 2013), global waters by 0.81 (Saulquin et al., 2019), and the West Sea of Korea has an R² of 0.939 – 0.996 (Mohebzadeh et al., 2020). Kriging can provide an excellent chlorophyll-a prediction model (Ha et al., 2013).

2.2.4 Data harmonization

SeaWiFS, Terra MODIS, and Aqua MODIS data obtained from different sensors will produce different reflectance values at the same wavelength, so harmonizing is necessary. Products of various sensors, such as Aqua MODIS and Terra MODIS, have different reflectance values due to different geometric and atmospheric conditions (Miura et al., 2021). For example, research in the Arabian Sea shows that the value of chlorophyll-a Aqua MODIS is higher than SeaWiFS by 25 – 32% in coastal eutrophic waters and lower by 25% in the open sea, as well as lower than Terra MODIS by 29–31% in the open ocean (Arun Kumar et al., 2015). Like the Landsat generation for NDVI, which has different acquisition conditions and sensors, it will produce reflectance inconsistencies in the same wave, so it is necessary to harmonize to compile time series data (Roy et al., 2016). Rrs 443, Rrs 555, and Rrs 670 are bands that need to be harmonized because they are used to calculate the chlorophyll-a global algorithm. The characteristics of the reflectance value of SeaWiFS and Terra MODIS are processed to have the same reflectance value characteristics as Aqua MODIS.

2.2.5 Calculation of the average value of chlorophyll-a

After obtaining the harmonized chlorophyll-a results, the average value of chlorophyll-a in the study area was calculated. Chlorophyll-a is sorted into a

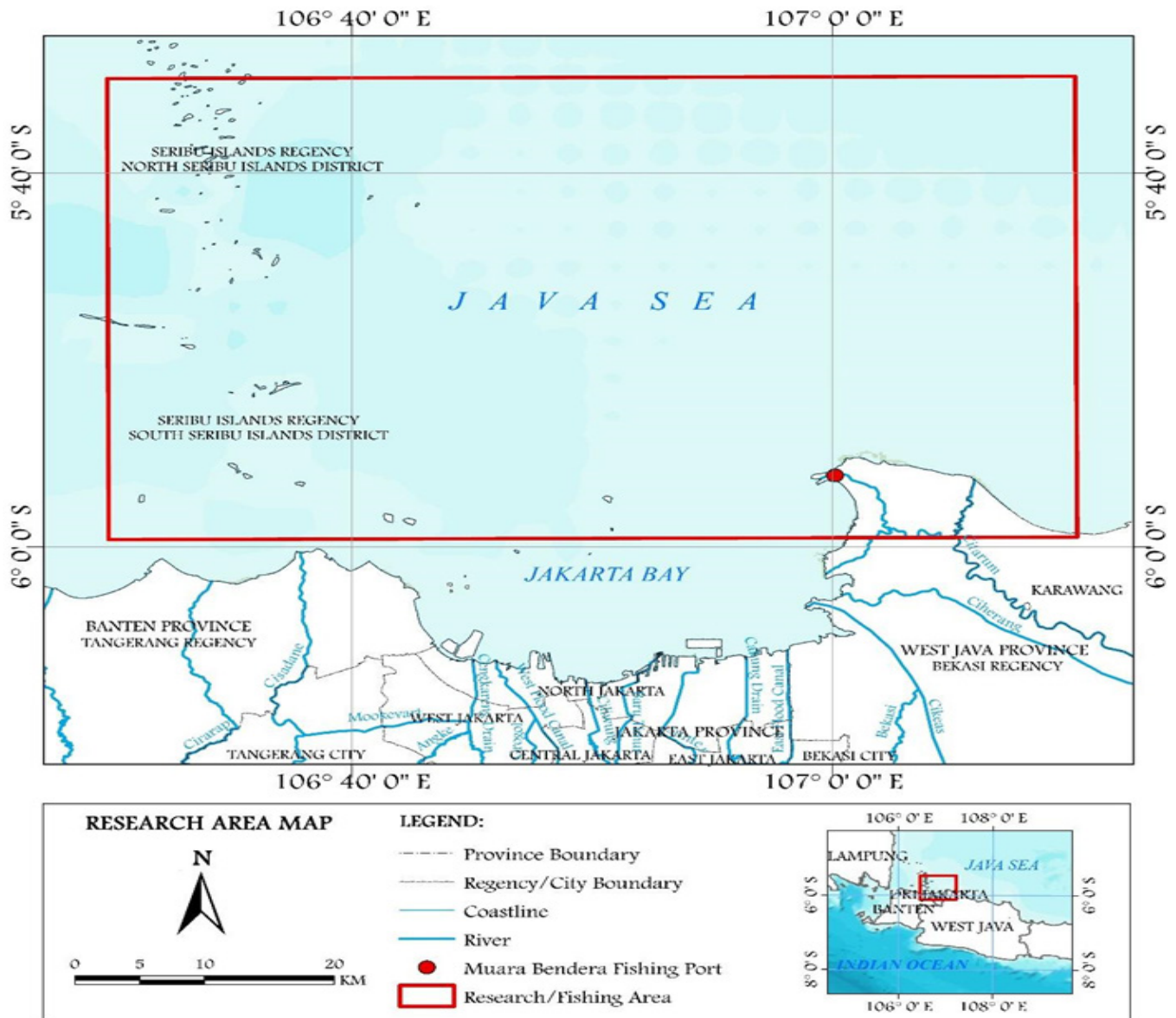


Figure 1. Research Area Map

monthly average by applying the following equation (Wirasatriya *et al.*, 2017):

$$X(x,y) = 1/n \sum_{i=1}^n x_i(x,y,t) \dots \dots \dots (ii)$$

Where :

$\bar{X}_{x,y}$ = the average value of the monthly chlorophyll-a data at the position (x, y)

x_i = the i th value of the data at the position (x, y)

t = the time t

n = the amount of data in one month

If x_i has a hollow pixel, that pixel is not included in the calculation.

2.2.6 Time series decomposition

A time series is a series of observational data arranged sequentially across time (Casolaro *et al.*, 2023). When the time series data are parsed, there are

main components, namely: Trends are general or non-linear (most frequent) systematic linear components that change over time and do not recur; Seasonality is a nonlinear (most frequent) systematic linear component that changes over time and repeats, usually within a year; meanwhile, random components are non-systematic trends and seasonality. In the adaptive time series model, there are four main components:

$$Y_t = S_t + T_t + R_t \dots \dots \dots (iii)$$

Where:

Y_t = the value of the time series in the period t

S_t = a seasonal component in the t period

T_t = a trend component in the t period

R_t is a reminder or fault component in the t period

If the time series monthly chlorophyll-a average value has an empty value, it is necessary to interpolate to get the full-time series data.

2.2.7 Spatial trend model

The non-parametric Mann-Kendall trend test was applied to identify linear trends in the monthly Chl-a time series (Colella et al., 2016). The magnitude of the slope was determined using the Sen method, where it was shown to have a significantly skewed distribution of Chl-a values and strong serial autocorrelations in the monthly Chl-a time series (Saulquin et al., 2013). The analysis of this model is for each pixel. The trend (β) is the median of the individual slope of each monthly sub-sample:

$$\beta = \text{median} [(X_{jm} - X_{im}) / (j - i)] \dots \dots \dots (iv)$$

Where :

the trend is expressed as the slope of chlorophyll-a, change per year (unit: mg/m³/year) (Wang et al., 2021).

2.3 Analysis Data

The purpose of simple linear regression analysis is to evaluate a free variable's relative impact on a bound variable. A simple linear regression model with one independent variable can be written using the following equation:

$$Y_i = a + bX_i + e_i \dots \dots \dots (v)$$

Where :

Y_i = a dependent variable

a = an intercept

b = a slope,

X_i = an independent variable

e_i is a relative error not correlated assumed.

The relationship between chlorophyll-a and the catch productivity of pelagic fish was calculated using the Pearson correlation test:

$$r = \frac{\sum xy - ((\sum x)(\sum y) / n)}{((\sum x^2 - ((\sum x)^2 / n)) - (\sum y^2 - ((\sum y)^2 / n)) \dots \dots \dots (vi)}$$

Where :

r = the correlation coefficient,

x = the average value of chlorophyll-a (independent variable)

y = the CPUE of pelagic (dependent variable)

The degree of correlation based on the correlation value includes very low (0 - 0.29), low (0.3 - 0.49), medium (0.5 - 0.69), strong (0.7 - 0.89), and very strong (0.9 - 1).

3. Results and Discussion

3.1 Spatial Distribution of Chlorophyll-a

The result showed the median value of chlorophyll-a over the three periods has the same pattern,

i.e., the highest concentration is at the mouth of the river, and the further away from the mouth of the river and the coast, the concentration decreases (Figure 2). The highest concentration is in the interior part of Jakarta Bay. In the central part of Jakarta Bay, the chlorophyll-a concentration is lower than in the Citarum River Estuary and the Cisadane Estuary to the east and west, respectively. Chlorophyll-a around the estuary had a median value of >2 mg/m³ from 2001 - 2021. This could be because river estuaries are places where nutrients from rivers meet seawater, creating conditions that are very suitable for the growth of phytoplankton, which is the main source of chlorophyll-A in waters. Shallow waters such as estuaries and coasts tend to have a high concentration of chlorophyll-a because there is a process of nutrient supply from rivers, and a mixing process occurs (Muskananfolia et al., 2021). Aside from that, river water carries sediment and organic material, which can supply additional nutrients to phytoplankton. As a result, chlorophyll-A concentrations are typically elevated around river mouths. In the interior of Jakarta Bay, nutrient sources may come from other factors, such as upwelling or thermal stratification, that influence local oceanographic conditions. These differences cause variations in chlorophyll-a concentrations at different locations within the bay. Dense contour intervals surround estuaries and shorelines for every 0.25 mg/m³ increment. This phenomenon demonstrates that chlorophyll-a concentrations are highest near estuaries and the coast, gradually decreasing toward the sea. High nutrition is always around the estuary, while offshore nutrition is rapidly declining (Damar et al., 2019).

Eutrophication rates in coastal waters based on chlorophyll-a values are divided into four groups: oligotrophic (<2 mg/m³), mesotrophic (2 - 6 mg/m³), eutrophic (6 - 20 mg/m³), and hypertrophic (>20 mg/m³) (Håkanson et al., 2007). The highest chlorophyll-a median value was in the interior of Jakarta Bay, namely around the East Flood Canal Estuary, Cakung Drain, and Sunter River at 41.71 mg/m³, and occurred in February 2003. The water of Jakarta Bay is eutrophic-hypertrophic waters. Meanwhile, the highest chlorophyll-a median value around the Citarum Estuary of 9.31 mg/m³ occurred in March 2015, so the waters around the mouth of the Citarum River include mesotrophic-eutrophic waters.

3.2 Chlorophyll-a Trend in Fishing Area of Muara Bendera

The general data trend from 1997 to 2021 shows an overall increase in chlorophyll-a concentrations in pelagic fishing areas. The harmonized chlorophyll-a monthly median data are displayed in Figure 3. Over the 24 years, there was an average annual

increase of +0.013 mg/m³ in chlorophyll-a concentration, equating to a growth rate of 1.43% per year. The average chlorophyll-a concentration from 1997 to 2021 was recorded at 1.08 mg/m³. Notably, the chlorophyll-a concentration in 1997 started at 0.93 mg/m³ and rose to 1.24 mg/m³ by 2021. In October 1997, the median chlorophyll-a concentration stood at 0.45 mg/m³, indicating a significant increase over time. The highest monthly chlorophyll-a concentration observed was 3.07 mg/m³, recorded in February 2003. This upward trend in chlorophyll-a concentrations suggests potential changes in the ecosystem dynamics of pelagic fishing areas over the studied period.

ditions that promote phytoplankton growth, such as increased nutrient availability and optimal temperature regimes. These conditions could result from factors such as enhanced river runoff, coastal upwelling events, or changes in ocean circulation patterns. In the segments of 1997 – 2000 and 2013 – 2021, there was a significant increase in the value of chlorophyll-a. Conversely, the periods of stable or declining chlorophyll-a values, such as 2000-2004 and 2006-2009, could be influenced by environmental factors that limit phytoplankton productivity, such as nutrient depletion, unfavorable temperature regimes, or changes in light availability. Anthropogenic influences, including

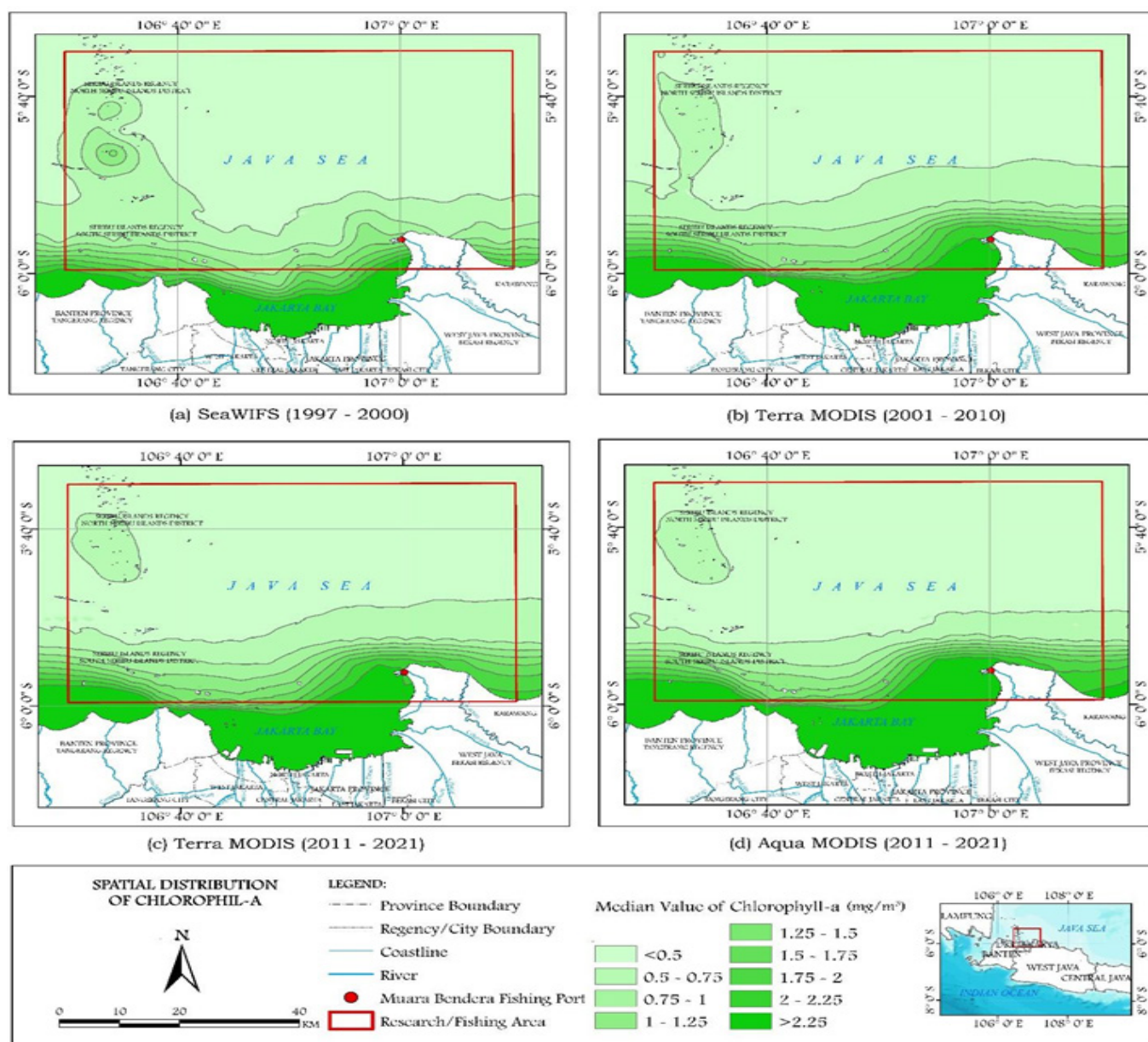


Figure 2. Spatial Distribution of Chlorophyll-a

The trend component shows that from 1997 – 2021, chlorophyll-a generally increased (Figure 4), which may be associated with favorable environmental con-

ditions that promote phytoplankton growth, such as increased nutrient availability and optimal temperature regimes. Pollution from urban and agricultural runoff

can introduce excess nutrients into marine environments, leading to eutrophication and algal blooms, which may contribute to increased chlorophyll-a concentrations during certain periods. Figure 5 indicates that in the rainy season, the highest chlorophyll-a values occur in February, and the lowest in April. In the dry season, the highest chlorophyll values occur in July and the lowest in October.

3.3 Spatial Trend Model of Chlorophyll-a

The result of the study showed that in 1997 – 2000, almost the entire region experienced an increase in the chlorophyll-a trend of 91.98% of the total fishing area (Figure 5). The increase in chlorophyll-a

of the waters of the Cisadane River Estuary from 2011 to 2021. The waters around the Citarum River Estuary and the Cisadane River Estuary consistently have an increasing trend every year from 1997 to 2021.

Since 2001, the waters of the North Seribu Islands have begun to experience an increasing trend, while the central part of Jakarta Bay has decreased. The waters of the South Seribu Islands in 2001 – 2010 experienced a decline, but in 2011 – 2021 they showed an increase. From 2001 – 2010, the chlorophyll values trend at the Citarum River's mouth increased by more than 0.02 mg/m³/year. Furthermore, from 2011 to 2021 the trend of chlorophyll-a values at the mouth of the Citarum River increased by 0.01 – 0.015 mg/m³/year.

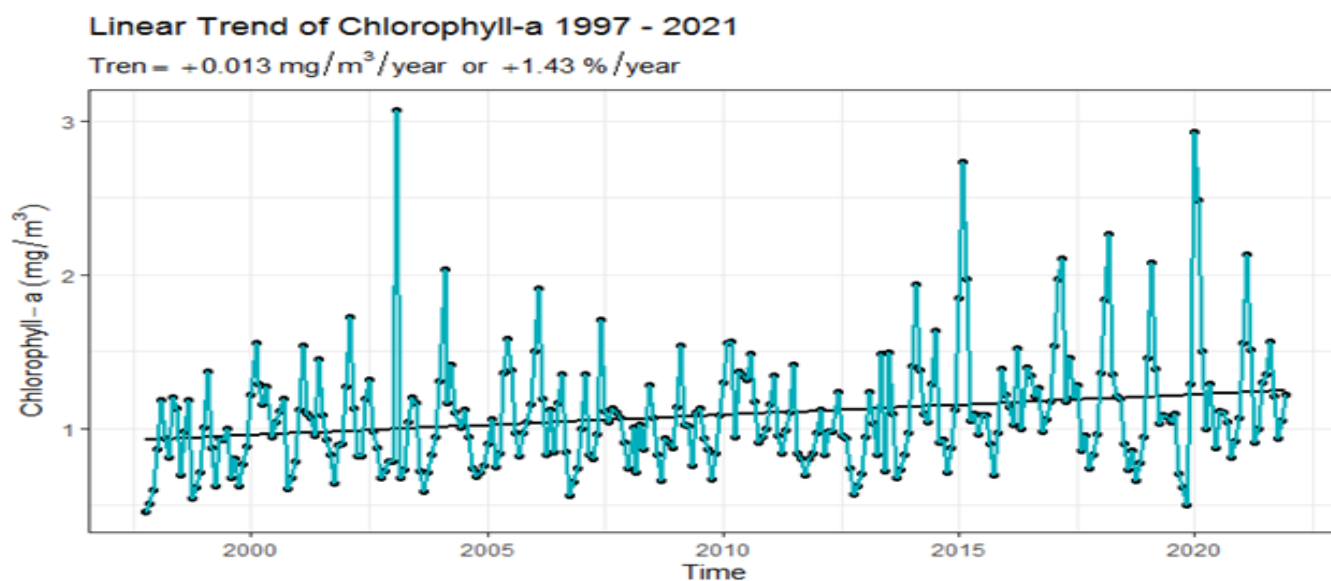


Figure 3. Linear of chlorophyll-a trend

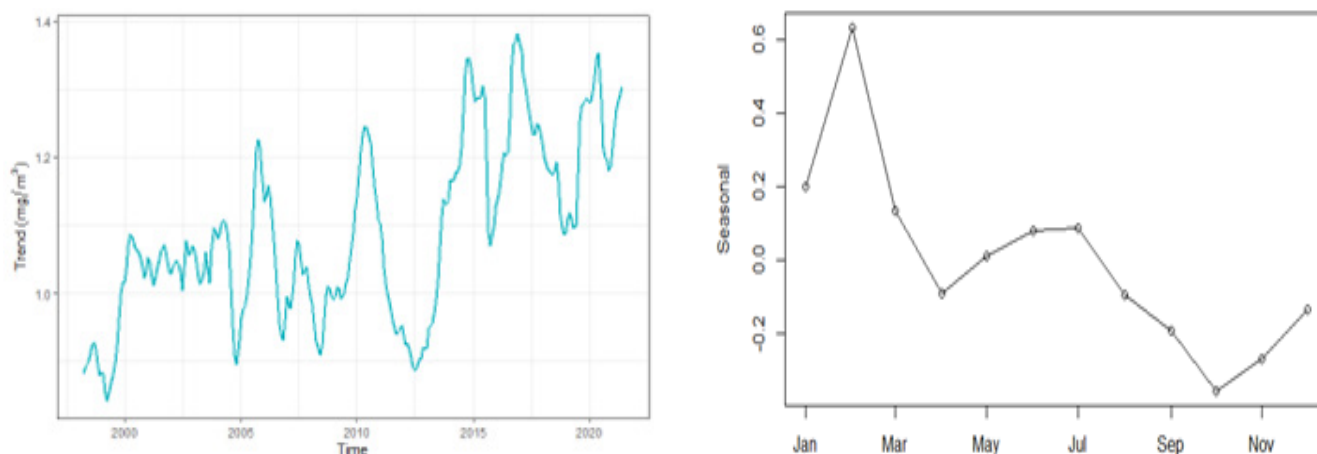


Figure 4. Chlorophyll-a: a) trend, and b) seasonal pattern

trend $>+0.02$ mg/m³/year covers an area of 72.97% of the total fishing area. The extent of the increased trend in 2011 – 2021 is larger than in 2001 – 2010, and this is consistent with the declining linear trend chart from 2006 to 2009. The area around the Citarum River Estuary that increased from 2001 to 2010 is larger than that

In 2001 – 2000, regions that experienced an increase in chlorophyll-a trend accounted for 60.08% of the total fishing area. A decrease or increase with a not very large value exists during this period. For example, areas that experience an increase in the trend of 0 to 0.005 mg/m³/year cover 27.16% of the total fishing

area. Another example is a region where the trend decreased from -0.005 to 0 $\text{mg}/\text{m}^3/\text{year}$, accounting for 28.65% of the fishing area.

From 2011 to 2021, the trend increased from Terra MODIS by 96.10% and Aqua MODIS by 93.93% of the total fishing area. The difference lies in the percentage

a small portion of the waters above the Citarum River Estuary has increased. In contrast, it has decreased in Aqua MODIS due to the different recording times. Terra MODIS and Aqua MODIS cross the equator at different times, namely 10:30 and 13:30, respectively (Frouin *et al.*, 2012).

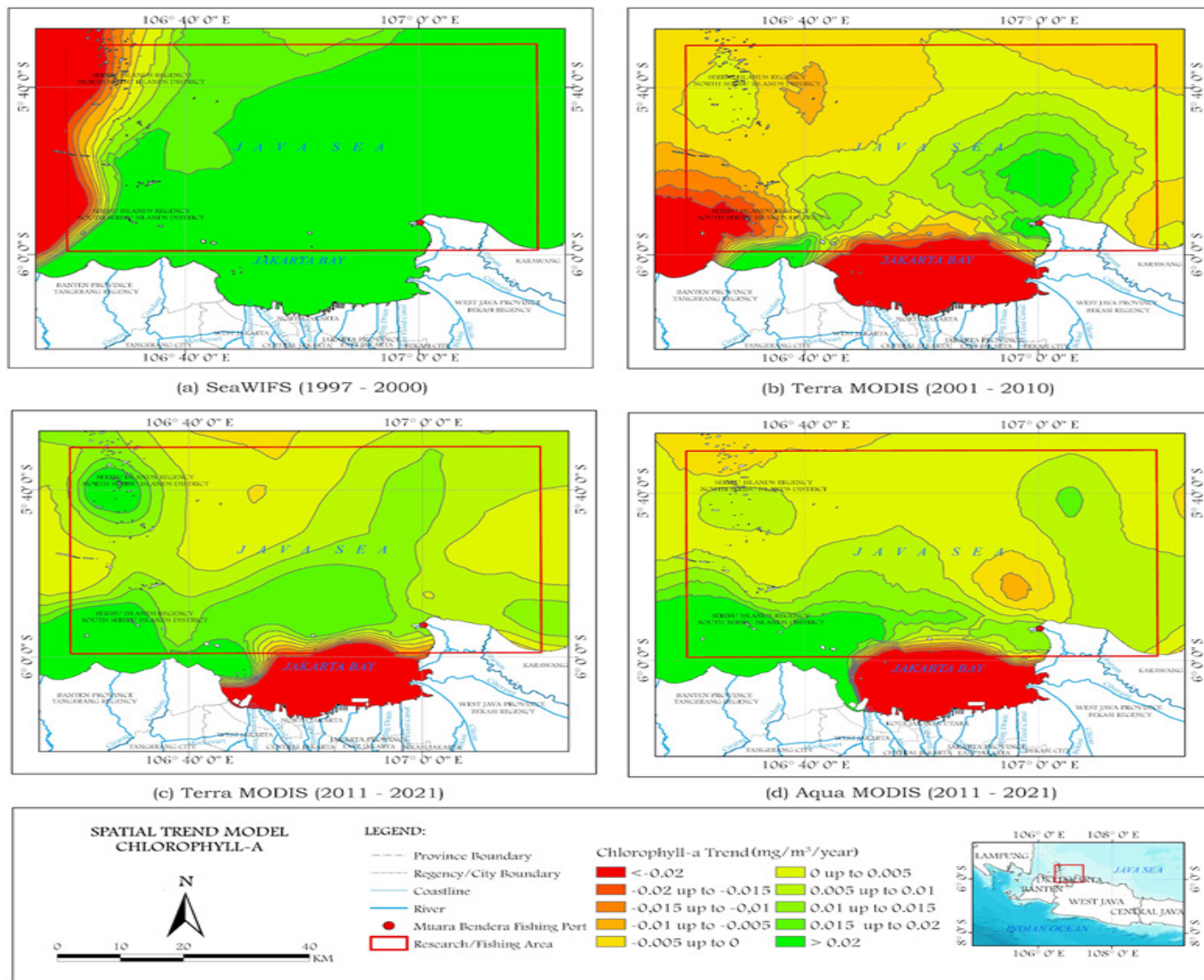


Figure. 5 Spatial trend model of chlorophyll-a

of the area of each trend class. The trend from Terra MODIS data, the most dominant class, is an increase of $0 - 0.005$ $\text{mg}/\text{m}^3/\text{year}$ and $0.005 - 0.01$ $\text{mg}/\text{m}^3/\text{year}$, respectively – an area of 24.68% and 31.61% of the total area of the fishing area. Meanwhile, for data from Aqua MODIS, the most dominant class is an increase of $0 - 0.005$ $\text{mg}/\text{m}^3/\text{year}$ and $0.005 - 0.01$ $\text{mg}/\text{m}^3/\text{year}$, covering an area of 40.26% and 30.56% of the total fishing area, respectively. The spatial trend of chlorophyll models-a Figure 6 (c) Terra MODIS and Figure 6 (d) Aqua MODIS exhibit almost the same spatial pattern. In addition, the Terra MODIS data indicate that the chlorophyll-a trend of

3.4 Relationship between chlorophyll-a and the CPUE of pelagic fish

The results of the correlation analysis in Figure 6 show chlorophyll-a and the CPUE of pelagic fish negatively correlated (-) or inversely proportional to -0.13 (very low). A negative correlation value (R) indicates that the upward trend of chlorophyll-a in the pelagic fishing area of the Muara Bendera was not offset by an increase in pelagic catches, instead indicating a decrease. Figure 7 shows the CPUE of Square-tail mullet and tuna has a negative correlation with chlorophyll-a of -0.11 and -0.04 , respectively. While

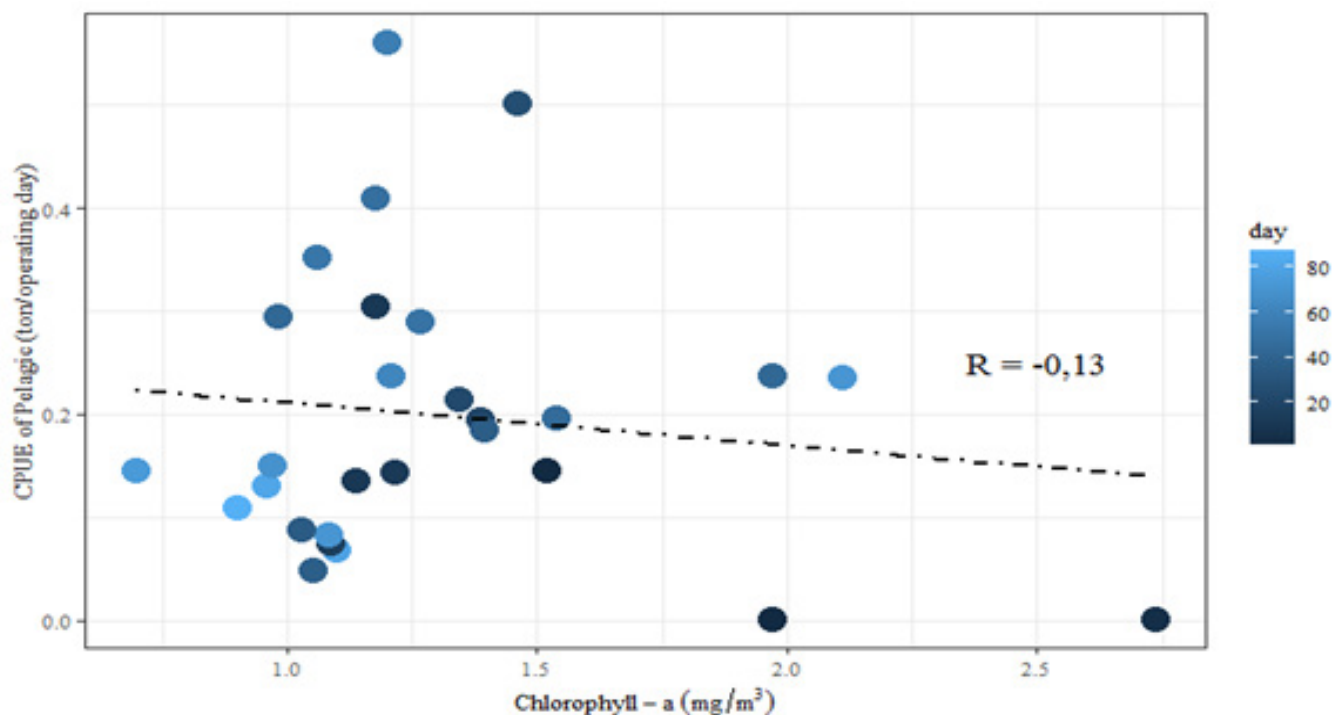


Figure 6. Correlation Analysis between Chlorophyll-a and CPUE of Pelagic

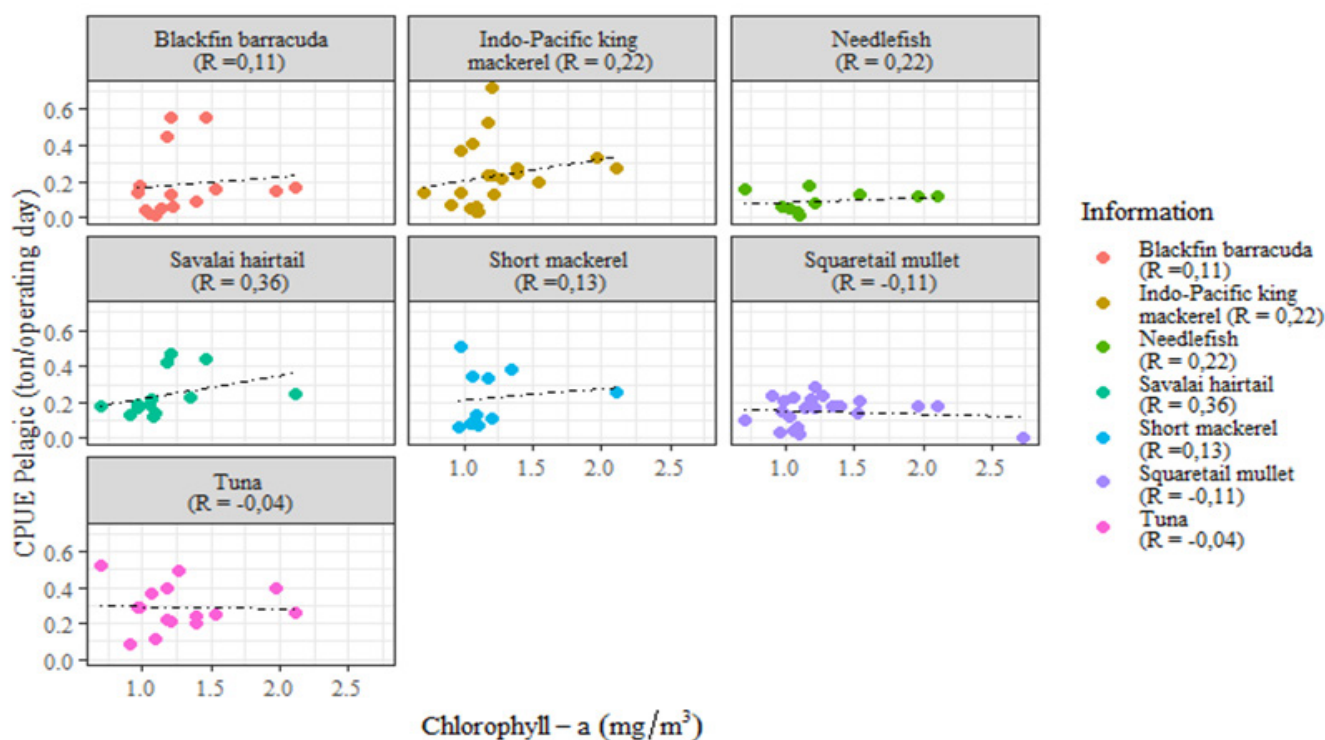


Figure 7. Correlation analysis between chlorophyll-a and CPUE of each pelagic

the CPUE of Blackfin barracuda, Short mackerel, Indo-Pacific king mackerel, Needlefish, and Savalai hairtail had a positive correlation with chlorophyll-a, which was 0.11 (very low); 0.13 (very low); 0.22 (very low); 0.22 (very low); and 0.36 (low) respectively.

3.5 Effect of ENSO phenomenon on CPUE of pe

logic fish

The result indicates that the maximum peak season of pelagic catch at the Muara Bendera Fishing Port occurs from October to December (Figure 8). There is a shift in the maximum peak of the of the catch, originally from December 2015, when

the El Nino phase was strong, to November 2016, when the La Nina phase was weak. The CPUE of pelagic fish is lower during the El Nino phase than during the weak or neutral La Nina, which is contrary to the theory that El Niño will increase the catch of pelagic fish due to the abundant availability of phytoplankton. However, The catches of some marine species are affected by El Niño (Alms and Wolff,

2020). The upwelling area is a fishing ground with high productivity (Hsiao *et al.*, 2021) because phytoplankton will utilize it (Paparazzo *et al.*, 2021). However there was no effect of ENSO on the CPUE of Muara Bendera pelagic fish because ENSO cannot evoke chlorophyll-a in this region. The ENSO only affects pelagic CPUE in large water areas such as oceans. The result also indicates an upward trend in the value of ONI in

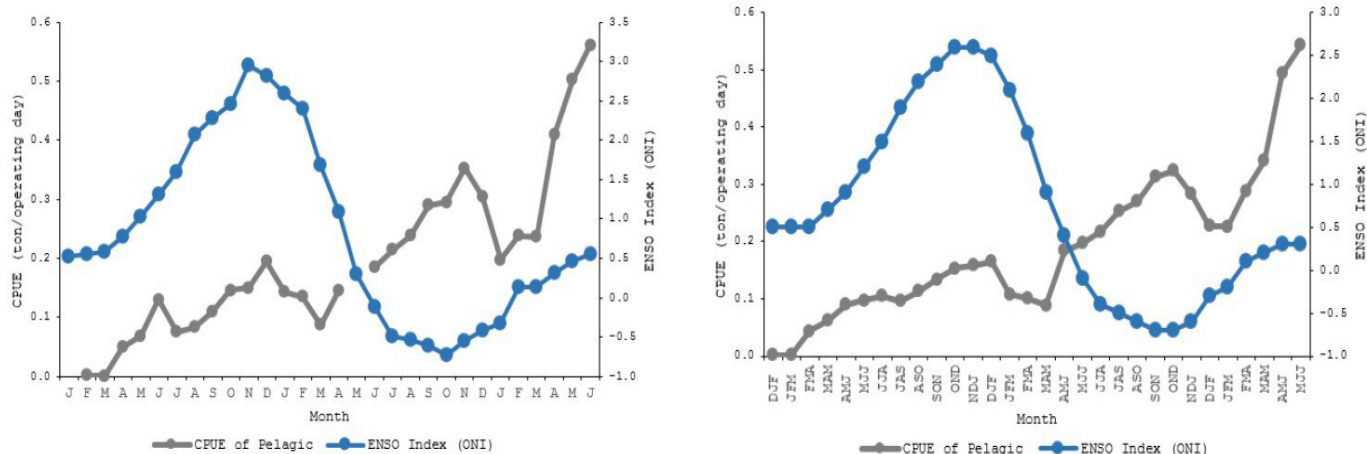


Figure 8. Graph the relationship between the ENSO index and pelagic CPUE of pelagic with monthly data (left) and quarterly data (right)

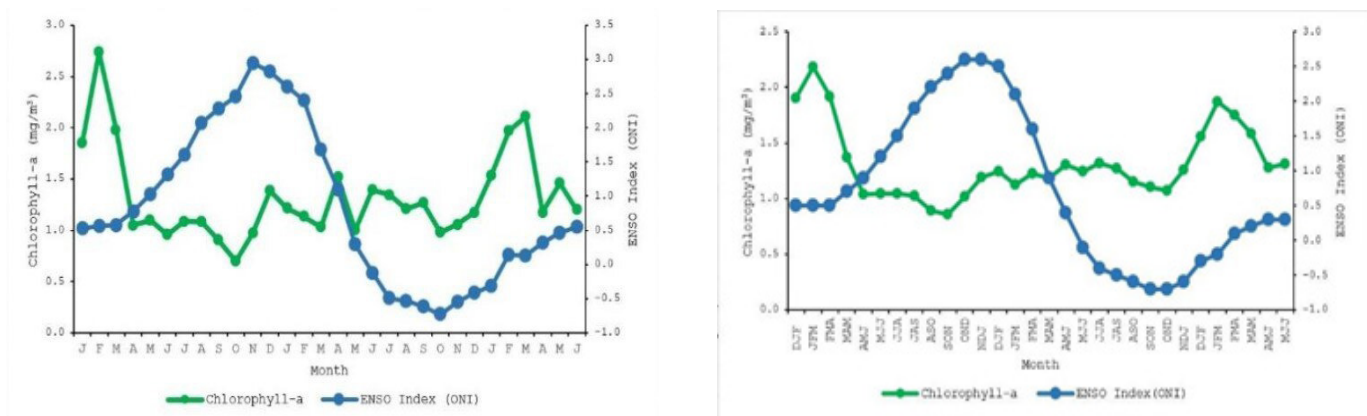


Figure 9. Graph the relationship between the ENSO index and chlorophyll-a with monthly data (left) and quarterly data (right)

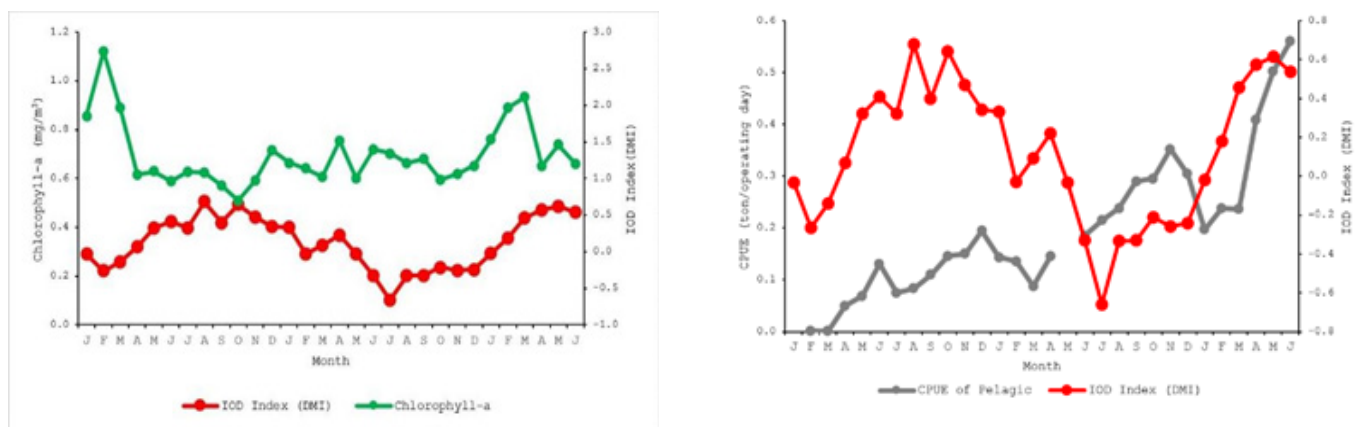


Figure 10. Graph the relationship between the IOD index and pelagic CPUE (Left) and relationship between IOD index and chlorophyll-a (right).

the weak to strong El Niño phase, not offset by an increase in the value of chlorophyll-a (Figure 9). ENSO has physical and physiological impacts on the Pacific Ocean and other oceanic basins through atmospheric teleconnection (Lehodey et al., 2020). For example, skipjack fish catches in the South Atlantic and Western Indian Oceans are closely related to the Northern Oscillation Index and the ENSO Index (Dahlet et al., 2019). ENSO dramatically affects pelagic fish populations but not as a major factor, and this dynamic is also influenced by continuously declining ocean conditions and fishing pressures (Lehodey et al., 2020).

3.6 Effect of IOD phenomenon on CPUE of pelagic fish

The result shows that the IOD index and CPUE have an almost similar trend (Figure 10). At the time of positive IOD, the DMI value gets bigger, which is always followed by an increase in the CPUE of pelagic fish. And vice versa. However, the same DMI values in different positive phases indicate a significant difference in CPUE values. The analysis continued by conducting a correlation analysis between DMI data and pelagic CPUE during the neutral to positive IOD phase. The results showed a positive correlation with the low category of 0.47. There has been no research on the effect of the IOD phenomenon on the productivity of pelagic catches in the Java Sea. In Indonesian waters, IOD significantly only affects pelagic catches in waters directly adjacent to the Indian Ocean, such as small pelagic in Pelabuhanratu Bay (Lumban-Gaol et al., 2021) and lemuru fish (*Sardinella lemuru* sp) in the Bali Strait (Setyohadi et al., 2021). Chlorophyll-a concentrations on the southern coasts of Java and west Sumatra are influenced by monsoon-driven upwelling and river discharge caused by rainfall in the Indian Ocean (Xu et al., 2021).

4. Conclusion

In conclusion, this research offers valuable insights for local governments working on sustainable fisheries. The increasing nutrient load in Jakarta Bay poses a threat to pelagic species by raising eutrophication levels. Proposed measures include stricter permits for industrial waste and improving river boundaries to reduce household waste. For the North Seribu Islands, a National Park, it's crucial to ban destructive fishing and limit sand/coral mining while promoting environmental awareness. Future research should use pelagic fish vessel data for the study area and longer-term productivity data for a comprehensive analysis. These recommendations aim to support sustainable fisheries and environmental preservation efforts.

Acknowledgement

This research was funded by the University of Indonesia through the International Indexed Publication Grant (PUTI) Q1 with the contact number on the grant NKB 415/UN2.RST/HKP.05.00/2024.

Authors' Contributions

The contribution of each author is as follows, Concept: MDMM, SUP; Data Collection: HS, Data Processing: HS; Writing and original draft preparation: MDMM and HS; Writing review and editing: MDMM. All authors have discussed and contributed to the final manuscript.

Conflict of Interest

The authors have no competing interests to disclose.

Funding Information

This research was funded by the University of Indonesia through the International Indexed Publication Grant (PUTI) Q1 with the contact number on the grant NKB-415/UN2.RST/HKP.05.00/2024.

References

- Ajani, P. A., Larsson, M. E., Woodcock, S., Rubio, A., Farrell, H., Brett, S., & Murray, S. A. (2018). Bloom drivers of the potentially harmful dinoflagellate *Prorocentrum minimum* (Pavillard) Schiller in a south eastern temperate Australian estuary. *Estuarine, Coastal and Shelf Science*, 215(16):161-171.
- Akram, H., Hussain, S., Mazumdar, P., Chua, K. O., Butt, T. E., & Harikrishna, J. A. (2023). Mangrove health: A review of functions, threats, and challenges associated with mangrove management practices. *Forests*, 14(9):1-38.
- Alms, V., & Wolff, M. (2020). Identification of drivers of change of the gulf of nicoya ecosystem (Costa Rica). *Frontiers in Marine Science*, 7(707):1-14.
- Apriansyah, Atmadipoera, A. S., Nugroho, D., Jaya, I., & Akhir, M. F. (2023). Simulated seasonal oceanographic changes and their implication for the small pelagic fisheries in the Java Sea, Indonesia. *Marine Environmental Research*, 188(6):1-51.
- Arun Kumar, S. V. V., Babu, K. N., & Shukla, A. K. (2015). Comparative analysis of chlorophyll-a distribution from SeaWiFS, MODIS-Aqua,

- MODIS-Terra and Meris in the Arabian Sea. *Marine Geodesy*, 38(1):40-57.
- Attila, J., Kauppila, P., Kallio, K. Y., Alasalmi, H., Keto, V., Bruun, E., & Koponen, S. (2018). Applicability of earth observation chlorophyll-a data in assessment of water status via MERIS — with implications for the use of OLCI sensors. *Remote Sensing of Environment*, 212(9):273-287.
- Casolaro, A., Capone, V., Iannuzzo, G., & Camastra, F. (2023). Deep learning for time series forecasting: advances and open problems. *Information*, 14(598):1-35.
- Ciancia, E., Coviello, I., Di Polito, C., Lacava, T., Pergola, N., Satriano, V., & Tramutoli, V. (2018). Investigating the chlorophyll-a variability in the Gulf of Taranto (North-Western Ionian Sea) by a multi-temporal analysis of MODIS-Aqua Level 3/Level 2 data. *Continental Shelf Research*, 155(4):34-44.
- Colella, S., Falcini, F., Rinaldi, E., Sammartino, M., & Santoleri, R. (2016). Mediterranean ocean colour chlorophyll trends. *Plos One*, 11(6):1-16.
- Dahlet, L. I., Downey-Breedt, N., Arce, G., Sauer, W. H. H., & Gasalla, M. A. (2019). Comparative study of skipjack tuna *Katsuwonus pelamis* (Scombridae) fishery stocks from the South Atlantic and Western Indian Oceans. *Scientia Marina*, 83(1):19-29.
- Damar, A., Hesse, K.-J., Colijn, F., & Vitner, Y. (2019). The eutrophication states of the Indonesian sea large marine ecosystem: Jakarta Bay, 2001–2013. *Deep Sea Research Part II: Topical Studies in Oceanography*, 163(5):72-86.
- Daqamseh, S., Al-Fugara, A., Pradhan, B., Al-Oraiqat, A., & Habib, M. (2019). MODIS derived sea surface salinity, temperature, and chlorophyll-a data for potential fish zone mapping: West Red Sea coastal areas, Saudi Arabia. *Sensors*, 19(9):1-25.
- Devlin, M., & Brodie, J. (2023). Nutrients and eutrophication. In A. Reichelt-Brushett (Ed.), *Marine pollution - monitoring, management and mitigation*. (pp. 75-100). Springer.
- Frouin, R., McPherson, J., Ueyoshi, K., & Franz, B. A. (2012, October). A time series of photosynthetically available radiation at the ocean surface from SeaWiFS and Modis data. *Proceedings of SPIE - The International Society for Optical Engineering*.
- Fu, Y., Xu, S., Zhang, C., & Sun, Y. (2018). Spatial downscaling of Modis chlorophyll-a using Landsat 8 images for complex coastal water monitoring. *Estuarine, Coastal and Shelf Science*, 209(10):149-159.
- Ghosh, S., Chatterjee, S., Shiva Prasad, G., & Pal, P. (2021). Effect of climate change on aquatic ecosystem and production of fisheries. In M. M. Shah, J. Pan, & A. Devlin (Eds.), *Inland waters - dynamics and ecology*. (pp. 1-11).
- Ha, N., Koike, K., & Nhuan, M. (2013). Improved accuracy of chlorophyll-a concentration estimates from MODIS imagery using a two-band ratio algorithm and geostatistics: As applied to the monitoring of eutrophication processes over Tien Yen Bay (Northern Vietnam). *Remote Sensing*, 6(1):421-442.
- Håkanson, L., Bryhn, A. C., & Blenckner, T. (2007). Operational effect variables and functional ecosystem classifications – a review on empirical models for aquatic systems along a salinity gradient. *International Review of Hydrobiology*, 92(3):326-357.
- Haridhi, H. A., Nanda, M., Haditjar, Y., & Rizal, S. (2018). Application of Rapid Appraisals of Fisheries Management System (RAFMS) to identify the seasonal variation of fishing ground locations and its corresponding fish species availability at Aceh Waters, Indonesia. *Ocean & Coastal Management*, 154(4):46-54.
- Hsiao, P.-Y., Shimada, T., Lan, K.-W., Lee, M.-A., & Liao, C.-H. (2021). Assessing summertime primary production required in changed marine environments in upwelling ecosystems around the Taiwan Bank. *Remote Sensing*, 13(4):1-22.
- Hu, C., Feng, L., & Guan, Q. (2021). A machine learning approach to estimate surface chlorophyll a concentrations in global oceans from satellite measurements. *IEEE Transactions on Geoscience and Remote Sensing*, 59(6):4590-4607.
- Hu, C., Lee, Z., & Franz, B. (2012). Chlorophyll a algorithms for oligotrophic oceans: A novel approach based on three-band reflectance difference. *Journal of Geophysical Research: Oceans*, 117(1):1-25.
- Ihsan, Y. N., Fellatami, K., Pasaribu, B., & Pribadi, T. D. K. (2023). Nutrient variability, pollution, and trophic status in Muara Gembong, Bekasi. *AACL Bioflux*, 16(3):1669-1681.
- Jakobsen, H. H., & Markager, S. (2016). Carbon-to-chlorophyll ratio for phytoplankton in

temperate coastal waters: Seasonal patterns and relationship to nutrients. *Limnology and Oceanography*, 61(5):1853-1868.

- James, N. C., Leslie, T. D., Potts, W. M., Whitfield, A. K., & Rajkaran, A. (2019). The importance of different juvenile habitats as nursery areas for a ubiquitous estuarine-dependent marine fish species. *Estuarine, Coastal and Shelf Science*, 226(11):1-18.
- Lehodey, P., Bertrand, A., Hobday, A. J., Kiyofuji, H., McClatchie, S., Menkès, C. E., Pilling, G., Polovina, J., & Tommasi, D. (2020). ENSO Impact on Marine Fisheries and Ecosystems. In M. J. McPhaden, A. Santoso, W. Cai (Eds.), *El Niño Southern oscillation in a changing climate*. (pp. 429-451). American Geophysical Union.
- Lumban-Gaol, J., Siswanto, E., Mahapatra, K., Natih, N. M. N., Nurjaya, I. W., Hartanto, M. T., Maulana, E., Adrianto, L., Rachman, H. A., Osawa, T., Rahman, B. M. K., & Permana, A. (2021). Impact of the strong downwelling (upwelling) on small pelagic fish production during the 2016 (2019) negative (positive) Indian Ocean dipole events in the Eastern Indian Ocean off Java. *Climate*, 9(2):1-29.
- Miura, T., Smith, C. Z., & Yoshioka, H. (2021). Validation and analysis of Terra and Aqua MODIS, and SNPP VIIRS vegetation indices under zero vegetation conditions: A case study using Railroad Valley Playa. *Remote Sensing of Environment*, 257(6):1-19.
- Mohebzadeh, H., Yeom, J., & Lee, T. (2020). Spatial downscaling of MODIS chlorophyll-a with genetic programming in South Korea. *Remote Sensing*, 12(9):1-19.
- Mukhtar, M. K., Supriatna, & Manessa, M. D. M. (2021). The validation of water quality parameter algorithm using Landsat 8 and Sentinel-2 image in Palabuhanratu Bay. *IOP Conference Series: Earth and Environmental Science*, 846(2):1-10.
- Muskananfolo, M. R., Jumsar, & Wirasatriya, A. (2021). Spatio-temporal distribution of chlorophyll-a concentration, sea surface temperature and wind speed using aqua-modis satellite imagery over the Savu Sea, Indonesia. *Remote Sensing Applications: Society and Environment*, 22(2):1-18.
- Nastiti A. S., Mujiyanto, & Krismono. (2020). The abundance of *Chaetoceros* spp. and its relation to the water quality parameters in the Muara Gembong Waters, West Jawa. *Jurnal Biologi Indonesia*, 16(1):39-46.
- Niu, L., Luo, X., Hu, S., Liu, F., Cai, H., Ren, L., Ou, S., Zeng, D., & Yang, Q. (2020). Impact of anthropogenic forcing on the environmental controls of phytoplankton dynamics between 1974 and 2017 in the Pearl River estuary, China. *Ecological Indicators*, 116(9):1-19.
- Paparazzo, F. E., Martinez, R. P., Fabro, E., Gonçalves, R. J., Crespi-Abril, A. C., Soria, G. R., Barbieri, E. A., & Almandoz, G. O. (2021). Relevance of sporadic upwelling events on primary productivity: The key role of nitrogen in a gulf of SW Atlantic Ocean. *Estuarine, Coastal and Shelf Science*, 249(2):1-16.
- Pitcher, G. C., & Jacinto, G. S. (2020). Ocean deoxygenation links to harmful algal blooms. In: D. Laffoley, & J. M. Baxter (Eds.), *Ocean deoxygenation: Everyone's problem. Causes, impact, consequences and solution*. (pp.153-170). Gland, Switzerland: International Union for Conservation of Nature (IUCN).
- Poddar, S., Chacko, N., & Swain, D. (2019). Estimation of chlorophyll-a in Northern Coastal Bay of Bengal Using Landsat-8 OLI and Sentinel-2 MSI Sensors. *Frontiers in Marine Science*, 6(598):1-11.
- Ramadhiani, A. F., & Suharyanto. (2021). Analysis of river water quality and pollution control strategies in the upper Citarum River. *IOP Conference Series: Earth and Environmental Science*, 623(2):1-8.
- Rodrigues, S. M., Almeida, C. M. R., Silva, D., Cunha, J., Antunes, C., Freitas, V., & Ramos, S. (2019). Microplastic contamination in an urban estuary: Abundance and distribution of microplastics and fish larvae in the Douro estuary. *Science of The Total Environment*, 659(16):1071-1081.
- Roy, D. P., Kovalskyy, V., Zhang, H. K., Vermote, E. F., Yan, L., Kumar, S. S., & Egorov, A. (2016). Characterization of Landsat-7 to Landsat-8 reflective wavelength and normalized difference vegetation index continuity. *Remote Sensing of Environment*, 185(14):57-70.
- Saulquin, B., Fablet, R., Mangin, A., Mercier, G., Antoine, D., & d'Andon, O. F. (2013). Detection of linear trends in multisensor time series in the presence of autocorrelated noise: Application to the chlorophyll-a SeaWiFS and MERIS data sets and extrapolation to the incoming Sentinel 3-OLCI mission. *Journal of Geophys-*

- ical Research: Oceans, 118(8):3752-3763.
- Saulquin, B., Gohin, F., & d'Andon, O. F. (2019). Interpolated fields of satellite-derived multi-algorithm chlorophyll-a estimates at global and European scales in the frame of the European Copernicus-Marine Environment Monitoring Service. *Journal of Operational Oceanography*, 12(1):47-57.
- Seegers, B. N., Stumpf, R. P., Schaeffer, B. A., Loftin, K. A., & Werdell, P. J. (2018). Performance metrics for the assessment of satellite data products: an ocean color case study. *Optics Express*, 26(6):7404-7422.
- Sembiring, E., Fareza, A. A., Suendo, V., & Reza, M. (2020). The presence of microplastics in water, sediment, and milkfish (*Chanos chanos*) at the downstream area of Citarum River, Indonesia. *Water, Air, and Soil Pollution*, 231(7):1-14.
- Ser-Giacomi, E., Zinger, L., Malviya, S., De Vargas, C., Karsenti, E., Bowler, C., & De Monte, S. (2018). Ubiquitous abundance distribution of non-dominant plankton across the global ocean. *Nature Ecology & Evolution*, 2(8):1243-1249.
- Setyohadi, D., Zakiyah, U., Sambah, A. B., & Wijaya, A. (2021). Upwelling Impact on *Sardinella lemuru* during the Indian Ocean dipole in the Bali Strait, Indonesia. *Fishes*, 6(8):1-9.
- Sholeh, M., Pranoto, P., Budiastuti, S., & Sutarno, S. (2018). Analysis of Citarum River pollution indicator using chemical, physical, and bacteriological methods. *AIP Conference Proceedings*, 2049(1):1-9.
- Tangke, U., Laisouw, R., Umagap, W. A., & Darmawaty. (2021). Variability of chlorophyll-a concentration relation to fish catch of Indian mackerel in West Halmahera waters. *IOP Conference Series: Earth and Environmental Science*, 777(2):1-9.
- Tangke, U., & Senen, B. (2020). Distribution of sea surface temperature and chlorophyll-a concentration its correlation with small pelagic fish catch in Dodinga Bay. *IOP Conference Series: Earth and Environmental Science*, 584(2):1-9.
- Tweddle, J. F., Gubbins, M., & Scott, B. E. (2018). Should phytoplankton be a key consideration for marine management? *Marine Policy*, 97(11):1-9.
- Van Meerssche, E., & Pinckney, J. L. (2019). Nutrient loading impacts on estuarine phytoplankton size and community composition: Community-based indicators of eutrophication. *Estuaries and Coasts*, 42(2):504-512.
- Van Trijp, D. (2021). Fresh fish: Observation up close in late seventeenth-century England. *Notes and Records: The Royal Society Journal of the History of Science*, 75(3):311-332.
- Vanhellemont, Q., & Ruddick, K. (2021). Atmospheric correction of Sentinel-3/OLCI data for mapping of suspended particulate matter and chlorophyll-a concentration in Belgian turbid coastal waters. *Remote Sensing of Environment*, 256(5):1-18.
- Wang, Y., Yao, L., Chen, P., Yu, J., & Wu, Q. (2020). Environmental influence on the spatiotemporal variability of fishing grounds in the Beibu Gulf, South China Sea. *Journal of Marine Science and Engineering*, 8(957):1-12.
- Wang, Y., Tian, X., & Gao, Z. (2021). Evolution of satellite derived chlorophyll-a trends in the Bohai and Yellow Seas during 2002–2018: Comparison between linear and nonlinear trends. *Estuarine, Coastal and Shelf Science*, 259(12):1-15.
- Welliken, M. A., Melmambessy, E. H., Merly, S. L., Pangaribuan, R. D., Lantang, B., Hutabarat, J., & Wirasatriya, A. (2018). Variability chlorophyll-a and sea surface temperature as the fishing ground basis of mackerel fish in The Arufura Sea. *E3S Web of Conferences*, 73(1):1-5.
- Wirasatriya, A., Setiawan, R. Y., & Subardjo, P. (2017). The effect of ENSO on the variability of chlorophyll-a and sea surface temperature in the Maluku Sea. *IEEE Journal of Selected Topics in Applied Earth Observations and Remote Sensing*, 10(12):5513-5518.
- Xu, T., Wei, Z., Li, S., Susanto, R. D., Radiarta, N., Yuan, C., Setiawan, A., Kuswardani, A., Agustyadi, T., & Trenggono, M. (2021). Satellite-observed multi-scale variability of sea surface chlorophyll-a concentration along the south coast of the Sumatra-Java Islands. *Remote Sensing*, 13(2817):1-19.
- Yin, Z., Li, J., Huang, J., Wang, S., Zhang, F., & Zhang, B. (2021). Steady increase in water clarity in Jiaozhou Bay in the Yellow Sea from 2000 to 2018: Observations from MODIS. *Journal of Oceanology and Limnology*, 39(3):800-813.
- Yu, Y., Wang, P., Wang, C., & Wang, X. (2018). Optimal reservoir operation using multi-objective evolutionary algorithms for potential estuarine eutrophication control. *Journal of Environmental Management*, 223(19):758-770.